human eyes with diabetes, leading to a reduction in thickness of the nerve fiber layer. Consequently, it is important to clarify the pathogenesis of RGC death in DR, and develop a neuroprotective treatment to try to rescue RGCs in the early stages of the disease.

In response, we evaluated RGCs in a metabolic model of hyperglycemia, using mice fed a high fat diet (HFD) and given low doses of streptozotocin (STZ), in which low doses of STZ led to partial destruction of pancreatic beta cells and a HFD induced insulin resistance (Mu et al., 2006; Srinivasan et al., 2005). In particular, we examined the contribution of calpain and oxidative stress to hyperglycemia-induced RGC death in vivo and in vitro experiments, and investigated whether modification of the calpain state with a pharmacological inhibitor and or adding of antioxidants has the potential to be a therapeutic target for the treatment of neurodysfunction in patients with DR.

Calpains are a family of 14 calcium-regulated, intracellular cysteine proteases, which modulate cellular functions by limited, specific proteolysis (Huang and Wang, 2001). Expressed ubiquitously in the cytoplasm of mammalian cells, they play an important role in various cell processes, including cell proliferation, signal transduction and apoptosis (Perrin and Huttenlocher, 2002). Calpain-1 (μ-calpain; activated with μM Ca^{2+}) and calpain-2 (m-calpain; activated with mM Ca^{2+}) are the two major calpain isoforms (Goll et al., 2003). Calpains are activated by locally increased intracellular Ca^{2+} levels through calcium channels and intracellular stores (Camins et al., 2006), their domains will shift towards the protease core to form a compact structure (Hanna et al., 2008). It is also associated with the degradation of their substrates including α-fodrin that forms a backbone of the membrane skeleton (Nath et al., 1996), which triggers the apoptosis pathway (Stys and Jiang, 2002).

This makes inhibition of calpain signaling a therapeutic target for several pathological conditions, including DR. Levels of calpain are regulated by an endogenous specific inhibitor, calpastatin. It binds and inhibits calpain when calcium levels are high, but releases it when calcium levels fall (Hanna et al., 2007). Recently, an exogenous calpain inhibitor, SNJ-1945, which has shown a strong ability to penetrate the retinal blood barrier after oral administration (Shirasaki et al., 2005), was described to have a neuroprotective effect against retinal cell degeneration in rat and mouse glaucoma models (Oka et al., 2006; Ryu et al., 2011). In this study, we designed our experiment using mice lacking the gene for calpastatin and SNJ-1945 for investigating the role of calpain activation and possibility of neuroprotection under RGC loss induced by hyperglycemia.

On the other hand, clinical and experimental research in vivo and in vitro in recent years has documented that oxidative stress is a common cause of retinopathy (Hinokio et al., 1999; Pan et al., 2008; Sano et al., 1998). Itoh and his colleagues described how in non-oxidative stress conditions, NF-E2 related factor 2 (Nrf2), a transcriptive factor responsible for regulation of antioxidant response genes, is tethered in the cell cytoplasm by a molecule called Keap-1 and turned over rapidly by proteasomal degradation (Itoh et al., 1999). However, in response to oxidative stress, Nrf2 is stabilized, and relocates to the nucleus, finally activating antioxidant response genes. Therefore, we used mice lacking the Nrf2 gene to induce oxidative stress and evaluate the link between oxidative stress and calpain activation.

The main goal of this study was to develop a better means to identify, prevent and treat DR in its earlier stages rather than wait for the onset of vision-threatening vascular lesions.

Research design and methods

Animals

Adult (10 weeks) male C57BL/6 mice (SLC, Shizuoka, Japan), age- and sex-matched Nrf2 knockout (Nrf2 KO) mice (Itoh et al., 1997), and calpastatin knockout mice (CAST KO) (Takano et al., 2005) were used in this study. All animals were maintained and handled in accordance with the ARVO Statement for the Use of Animals in Ophthalmic and Vision Research and the guidelines from the Declaration of Helsinki and Guiding Principles in the Care and Use of Animals. All experimental procedures described in the present study were approved by the Ethics Committee for Animal Experiments at Tohoku University Graduate School of Medicine.

Mouse model of hyperglycemia

After 4 hr of fasting, hyperglycemia was induced by intraperitoneal injection of streptozotocin (STZ, 40 mg/kg body weight, Sigma, St. Louis, MO) or in the control group, citrate buffer, for five consecutive days. All the animals were fed a high fat diet (405.5 kcal energy, 24.2% protein, 13.6% fat, 3% fiber; Quick Fat, Clea, Japan, INC) at the time of STZ administration and throughout the experiment. Seven days after the first STZ treatment, SNJ-1945 (0.5 mL, 100 mg/kg) (Senju Pharmaceutical Co. Japan, Ltd.) or carboxymethylcellulose (CMC) was administered orally once a day until the animals were killed with an overdose of anesthesia. Blood was sampled from the tail vein and blood sugar was measured with a G-Checker (Gunze, Japan) before and after STZ treatment every week. Body weight was also recorded. Achievement of hyperglycemia was defined by a blood glucose level > 250 mg/dL 7-days after the last injection of STZ, and confirmed by measuring HbA_{1C} 4-weeks after the induction of hyperglycemia.

Retrograde labeling of RGCs and cell count

Retrograde labeling with fluorochrome (Fluorogold: FG, Englewood, CO) was performed as previously described by us (Nakazawa et al., 2007a). Briefly, the mice were anesthetized with a mixture of ketamine (100 mg/kg; Ketaset, Fort Dodge Animal Health, Fort Dodge, IA) and xylazine (9 mg/kg, TranquiVed; Vedco Inc., St. Joseph, MO) prepared at room temperature. Under full anesthesia, two small holes were drilled into the skull at the sites corresponding to the superior colliculi, where 2 μL of 2% FG with 1% dimethylsulfoxide (DMSO) was injected using a Hamilton syringe with a 32 G needle. Seven days after injection of FG, the mice were killed with an overdose of anesthesia; the retinas were harvested, and fixed with 4% of paraformaldehyde (PFA) overnight. The retinas were flat-mounted and the RGC density was determined by counting the FG-labeled RGCs in 12 distinct areas under the microscope (Axiovert-200; Zeiss, Germany) (Nakazawa et al., 2007a).

Quantitative RT-PCR (qRT-PCR)

qRT-PCR was performed as previously described (Nakazawa et al., 2007c) with minor modifications. Neural retinas were sampled and immediately sunk in an RNA stabilization reagent (RNase later, Sample and Assay Technology; Qiagen). Total RNA was extracted from the retinas using an extraction reagent (TRIzol; Invitrogen) and cDNA was synthesized with SuperScript III reverse transcriptase (Invitrogen). Real-time PCR was performed using a 7500 Fast Real Time PCR System (A&B Applied Biosystems, CA) with PCR primers for calpain-1 and calpain-2 designed by TaqMan Gene Expression Assays (Applied Biosystems, Foster, CA). The mRNA levels were normalized to GAPDH as an internal control.

Immunoblot assay

Immunoblotting was performed as previously described with one minor modification (Nakazawa et al., 2007b, 2008). The isolated retinas were placed in a lysis buffer (10 mmol/L Tris–HCl; pH 7.6, 100 mmol/L NaCl, 1 mmol/L EDTA, 1% Triton X-100, protease inhibitors). Each sample

was separated with SDS-PAGE and electroblotted to polyvinylidene fluoride membranes (Millipore, Bedford, MA). After blocking the membrane with 4% skim milk (Bio-Rad Laboratories), the membranes were incubated with a primary mouse monoclonal antibody against α-fodrin (1:1000, Abcam), or a polyclonal antibody against synaptophysin (1:1000, Cell Signaling) and β-tubulin (1:2000, Cell Signaling) overnight at 4 °C. The membranes were then incubated with a horseradish peroxidase-conjugated mouse immunoglobulin secondary antibody followed by avidin–biotin horseradish peroxidase complexes (Vectastain Elite ABC Kit; Vector, Burlingame, CA). The signals were visualized with chemo-luminescence (ECL Blotting Analysis System; Amersham, Arlington Heights, IL) measured by ImageJ software (Ver.1.44, Mac, US) and normalized to β-tubulin.

Immunohistochemistry

Immunohistochemistry (IHC) was performed as previously described (Nakazawa et al., 2007a, 2007b). Briefly, the retinal sections were incubated with a blocking buffer (PBS containing 10% goat serum, 0.5% gelatin, 3% bovine serum albumin, and 0.2% Tween 20) followed by a primary antibody against C38 (BM88) (Wakabayashi et al., 2010) or synaptophysin (1:200; Cell Signaling Technology, Inc.). The sections were then incubated with Alexa 488-conjugated goat anti-mouse or goat anti-rabbit IgG (1:200, Molecular Probes, Eugene) in a blocking buffer. The slides were shielded with a Vectashield mounting medium with DAPI (Vector Laboratories, Burlingame, CA). Photographs of the retina were taken using a

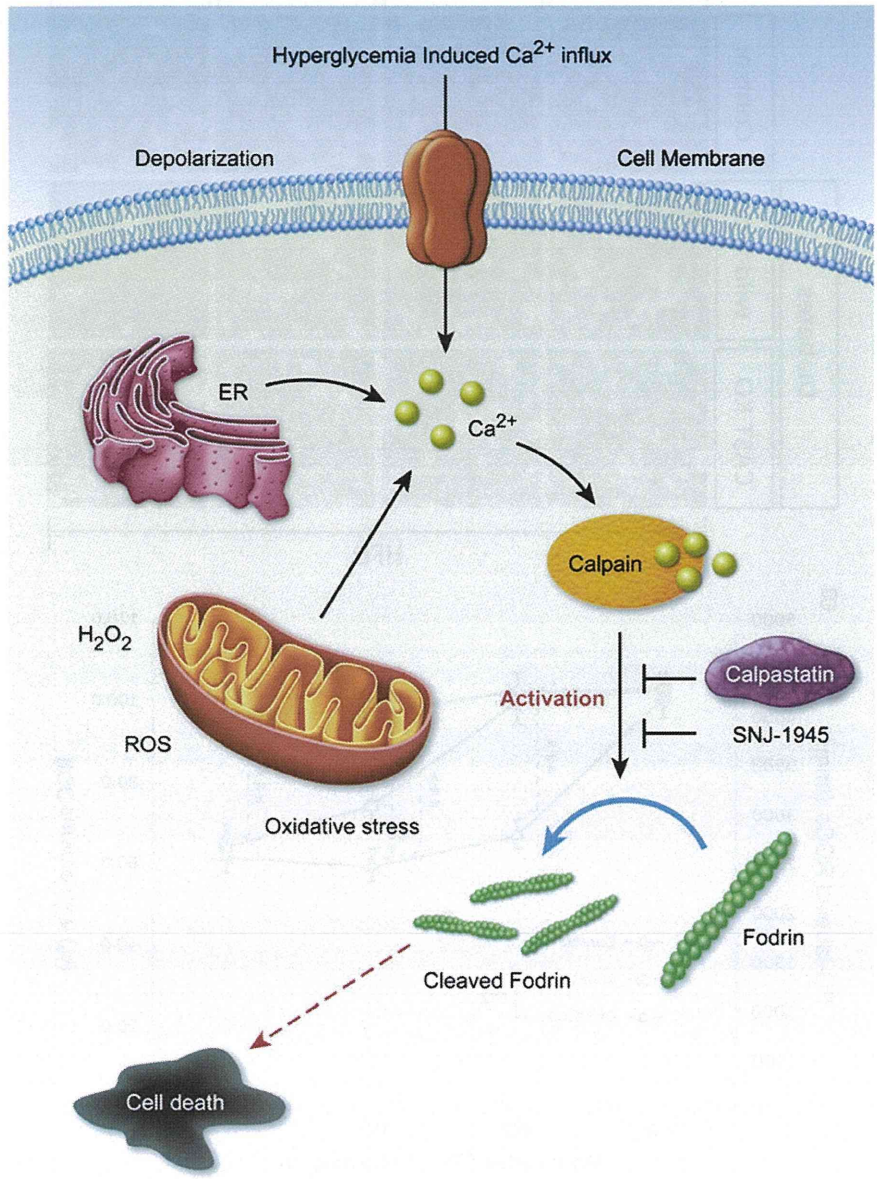

Fig. 1. Illustrative diagram showing the activation of the calpain pathway induced by Ca^{2+} ion influx overload. Hyper-excitability of the cell membrane due to hyperglycemia leads to cell membrane depolarization followed by a Ca^{2+} influx through the voltage sensitive Ca^{2+} channel. Once inside the cell, the excitation of ER and mitochondria through an increase in ROS, and the release of H_2O_2 hints at a release of more intracellular Ca^{2+}, reaching a millimolar level. Subsequently, calpain activation and cleavage leads to cell death. Calpastatin, an endogenous calpain inhibitor, showed the limitations of suppressing calpain activation. On the other hand, SNJ-1945, an exogenous calpain inhibitor, showed a more potential anti-apoptotic effect by suppressing calpain activation in the presence of a pathological intracellular Ca^{2+} level.

microscope equipped with fluorescence illumination (Axiovert-200; Zeiss, Germany).

Histological procedures for optic nerve axon analysis

To investigate the extent of hyperglycemia-induced axonal degeneration, 1 μm sections of optic nerve were processed as described in our previous publications (Nakazawa et al., 2006). Briefly, optic nerves were obtained from animals 4-weeks after STZ-induced hyperglycemia. For quantitative analyses, we analyzed five sections from each experimental condition. Optic nerves were placed immediately into a fixative consisting of 2.5% glutaraldehyde and 2% formaldehyde in 0.1 M cacodylate buffer with 0.08 M $CaCl_2$ overnight at 4 °C. The tissue was washed in 0.1 M cacodylate buffer and post-fixed in 2% aqueous OsO_4. Segments were dehydrated in graded alcohols and embedded in Epon. Then 1-μm sections were cut and stained with 1% toluidine blue in 1% borate buffer. Images were acquired using the 100× oily lens on a light microscope (BX51, Olympus) using a coupled digital camera (MP5Mc/OL, Olympus) and associated DP2-BSW software (Ver.1.3). The acquired images were quantified using Win ROOF software (Ver. 5.8.1). The number of axons was averaged per eye and expressed as numbers/mm^2.

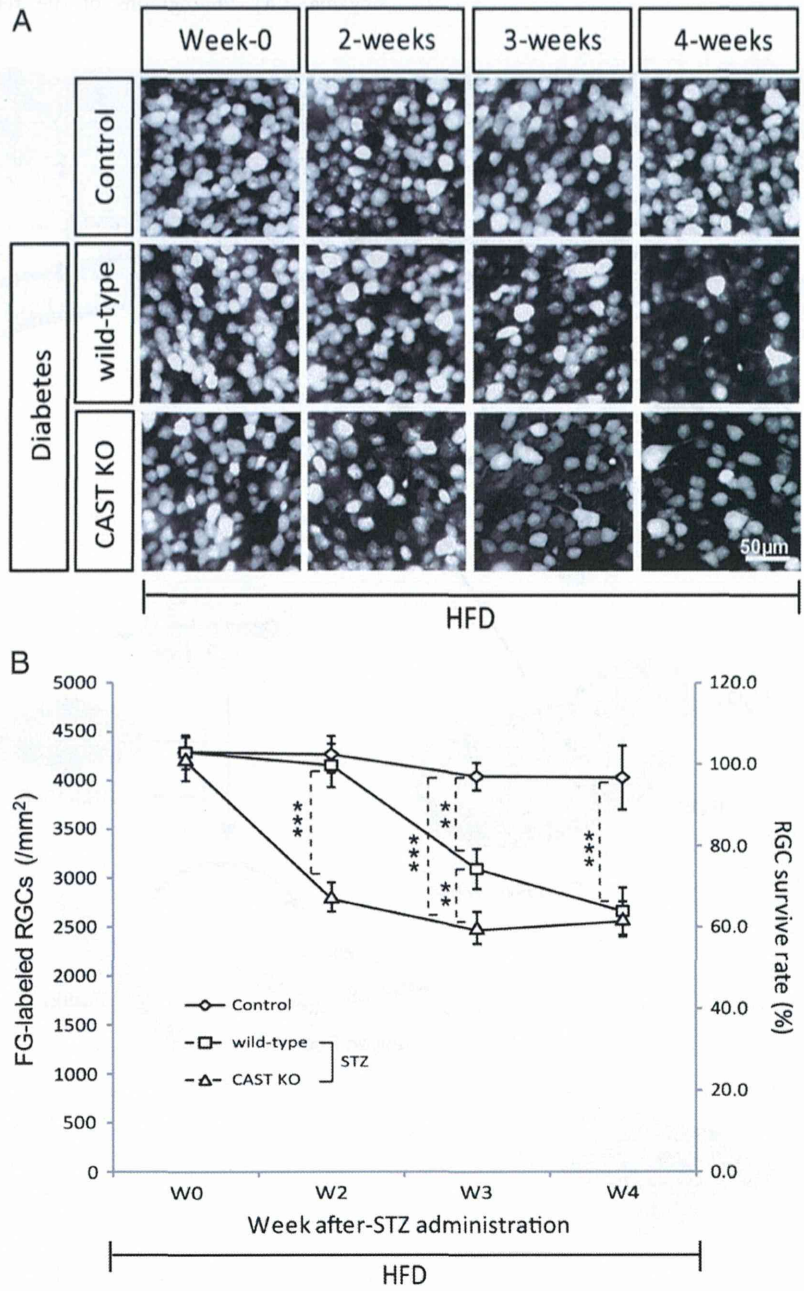

Fig. 2. Time course of fluorogold (FG)-labeled retinal ganglion cells (RGCs) with or without STZ treatment. (A) Representative photos of FG-labeled RGCs in flat-mounted retinas at four different time points (0 weeks: n = 8; two, three, and four weeks: n = 10 respectively). (B) Number of FG-labeled RGCs over time. The quantitative data of FG-labeled RGCs verified the earlier observation that the most significant degeneration was 2-weeks after STZ induction in CAST KO mice, compared to 3-weeks for wild-type mice. This showed the role of calpastatin as an endogenous calpain inhibitor and a limited delay in calpain activation in wild-type mice. Both showed around 38% RGC loss at the fourth week. **p<0.001, ***p<0.0001. Diamonds = control (citrate), squares = wild-type (STZ), triangles = CAST KO (STZ), HFD = high fat diet.

Adult mouse retinal primary cultures

Adult mouse primary retinal cultures were prepared as previously described with minor modifications (Nakazawa et al., 2007a, 2007c). Six neural retinas from 8-week-old mice were immediately dissected in Hank's buffered-saline solution (HBSS) and incubated at 37 °C for 10 min in a CO_2 incubator in a digestion solution containing papain (10 U/mL; Worthington, Lakewood, NJ) and L-cysteine (0.3 mg/mL; Sigma) in HBSS. Retinas were rinsed and triturated in HBSS containing bovine serum albumin (1 mg/mL; Sigma) and DNase (0.2 mg/mL; Sigma). Dissociated cells were passed through a strainer (40-μm nylon net; Falcon, Bedford, MA) and collected by centrifugation. Cells from six mouse retinas were resuspended in a 1 mL Neurobasal A medium (Invitrogen) with B27 supplement without antioxidants (NBA/B27AO−, 10889-038; Invitrogen). The density of retinal cells in the suspension was counted and the cells were seeded to each well of an 8-well chamber (4×10^4 cells per well, Nunc, Naperville, IL, USA). The total volume in each well was increased to 400 μL with NBA/B27AO− or NBA/B27AO+ (antioxidant cocktail = vitamin E, vitamin E acetate, superoxide dismutase, catalase and glutathione; B27, 17504-044; Invitrogen), 1 μg/mL insulin, 2 mM L-glutamate and 12 μg/mL gentamicin with or without 45 mM D-glucose. The cells were further incubated for 24 h with 5% CO_2 at 37 °C with or without 40 μM of SNJ-1945. Cells were then gently washed with PBS and fixed with 4% PFA for 10 min at room temperature. To assess the viability of RGCs, we performed immunocytochemistry (ICC) with mouse anti-βIII tubulin antibody, an RGC marker. The cells were permeabilized with 0.1% Triton X-100 in PBS for 5 min and incubated in a blocking buffer for 30 min at room temperature. Cells were then incubated with a monoclonal anti-βIII tubulin antibody (1:400 dilution, Sigma) at 4 °C overnight, rinsed (PBS 3×, 5 min), incubated with goat anti-mouse secondary antibody (1:200, Alexa Fluor-488; Molecular Probes, 1 hr at room temperature) and rinsed again (PBS 3×, 5 min). Eight-well chamber slides were mounted with a Vectashield mounting medium with DAPI. Controls were treated similarly, except without the primary antibody. Samples were arranged in a pseudo-randomized manner on the plates so that the investigator would not be aware of their identity when quantifying βIII tubulin-positive RGCs. To quantify the βIII tubulin-positive RGCs, 10 random images per well were captured using a fluorescent microscope (20× objective) equipped with a digital imaging system. Subsequently, the βIII tubulin-positive cells were counted using the IMAGEJ software. We repeated these cultures four times; values represent the mean ± SEM of four replicate wells.

Statistical analysis

All data were expressed as mean ± SD. The values were processed for statistical analysis with one-way ANOVA followed by Tukey's post hoc test (JMP, SAS institute, Mac ver.). Differences were considered statistically significant at $p<0.05$.

Results

Induction of hyperglycemia via HFD and STZ

Mice treated with STZ (40 mg/kg, 5 shots/5 days) and fed a HFD showed a significant decrease in body weight, increase in blood sugar levels, and levels of HbA_{1C} (S. Fig. 1). This was true for STZ-treated wild-type, CAST KO, and Nrf2 KO mice compared to age-matched citrate buffer control mice (S. Fig. 1A–D, B–E, C–F).

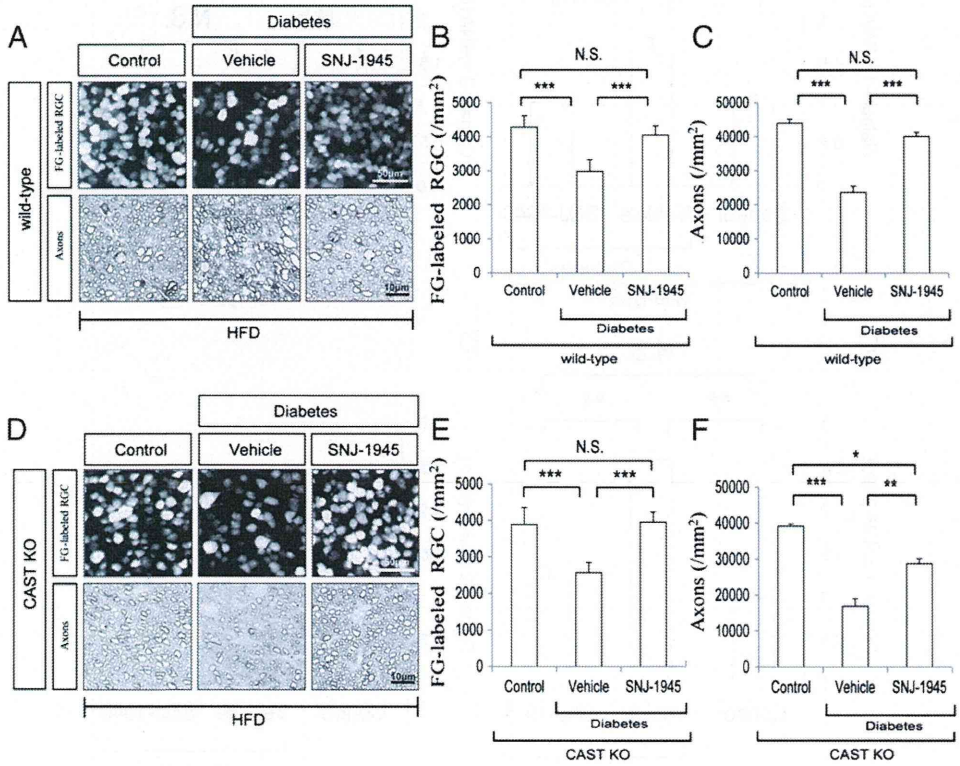

Fig. 3. SNJ-1945 prevented RGC and axonal degeneration in wild-type and CAST KO mice after four weeks of HFD- and STZ-induced hyperglycemia. (A, D upper panels) Representative photographs (wild-type and CAST KO mice, respectively) of FG-labeled RGCs in flat-mounted retinas with or without SNJ-1945 (100 mg/kg/wt). (A, D lower panels) Representative photographs (wild-type and CAST KO mice, respectively) of micro-sectioned samples of the optic nerve axons. (B, E) Bar charts showing quantitative data of the density of FG-labeled RGC in wild-type and CAST KO mice, respectively. (C, F) Bar charts showing quantitative data of axon density in the three different conditions, for wild-type and CAST KO mice, respectively. SNJ-1945 had a significant neuro-protective effect on HFD- and hyperglycemia-induced RGC death and axonal degeneration. N.S.: no significance. *$p<0.01$, **$p<0.001$, ***$p<0.0001$ vs. control.

HbA_{1C} was significantly higher in the mice treated with STZ or SNJ-1945 than in the control mice (S. Fig. 1G, H, I). These data suggest that modification of either calpastatin or Nrf2 does not influence HFD- and STZ-induced hyperglycemia.

HFD- and hyperglycemia-induced RGC death through calpain activation

To investigate the cytotoxic effects of HFD- and STZ-induced hyperglycemia, the density of surviving FG-labeled RGCs was verified at zero, two, three, and four weeks after STZ and in the control group, which received a citrate buffer treatment (Fig. 2). The control group (treated with citrate buffer) experienced no significant change in the density of positive FG-labeled RGCs, but the STZ-treated wild-type mice experienced a significant decrease in the density of FG-labeled RGCs beginning at 3-weeks (3092 ± 204 cells/mm^2, $p = 0.0002$) compared to the control (4041 ± 142 cells/mm^2) at the same time mark. RGC density continued to decline, and at 4-weeks, the percentage of RGCs that survived in the STZ-treated mice was 62.0% (2661 ± 240 cells/mm^2, $p<0.0001$) compared to the control mice (4031 ± 330 cells/mm^2). In STZ-treated CAST KO mice, interestingly, the time scale was different. After only 2-weeks, the density of RGCs was significantly lower (2807 ± 150 cells/mm^2, $p<0.0001$) than in the STZ-treated wild-type mice (4154 ± 222 cells/mm^2) (Fig. 2B). These data suggest that calpain plays an important role in the pathogenesis of RGC death in hyperglycemia-induced retinopathy, and that calpastatin, an endogenous calpain inhibitor, has a limited ability to suppress calpain activation in the retinas of the wild-type mice.

Calpain had a neurotoxic effect on HFD- and hyperglycemia-induced RGC death and axonal degeneration

To investigate whether calpain activation played a role in HFD- and hyperglycemia-induced degeneration of RGCs and their axons, we sampled the retina and optic nerve 4-weeks after STZ treatment. The density of positive FG-labeled RGCs was significantly lower (2985 ± 345 cells/mm^2, $p<0.0001$) in the wild-type mouse vehicle (STZ-CMC) group compared to the control group treated with citrate buffer (4289 ± 330 cells/mm^2). Orally administered SNJ-1945 significantly (4051 ± 269 cells/mm^2, $p<0.0001$) suppressed the degeneration of RGCs (Fig. 3A, upper panel, B) compared to the vehicle group. Concomitantly, axonal degeneration was significantly ($40{,}072 \pm 1192$ axon/mm^2, $p<0.0001$) suppressed in STZ-SNJ-1945 treated mice, compared to the vehicle group ($23{,}656 \pm 1798$ axon/mm^2) (Fig. 3A, lower panel, C). In the CAST KO mice, the density of RGCs degenerated significantly (2580 ± 271 cells/mm^2, $p<0.0001$) in the vehicle group compared to the control group mice (3890 ± 461 cells/mm^2). SNJ-1945 was also able to suppress the degeneration of RGCs (3959 ± 275 cells/mm^2, $p<0.0001$) (Fig. 3D, upper panel, E) and their axons ($28{,}742 \pm 1427$ axon/mm^2, $p<0.0001$) (Fig. 3D, lower panel, F) compared to the vehicle group. These data showed a coincident degeneration of both RGCs and their axons after

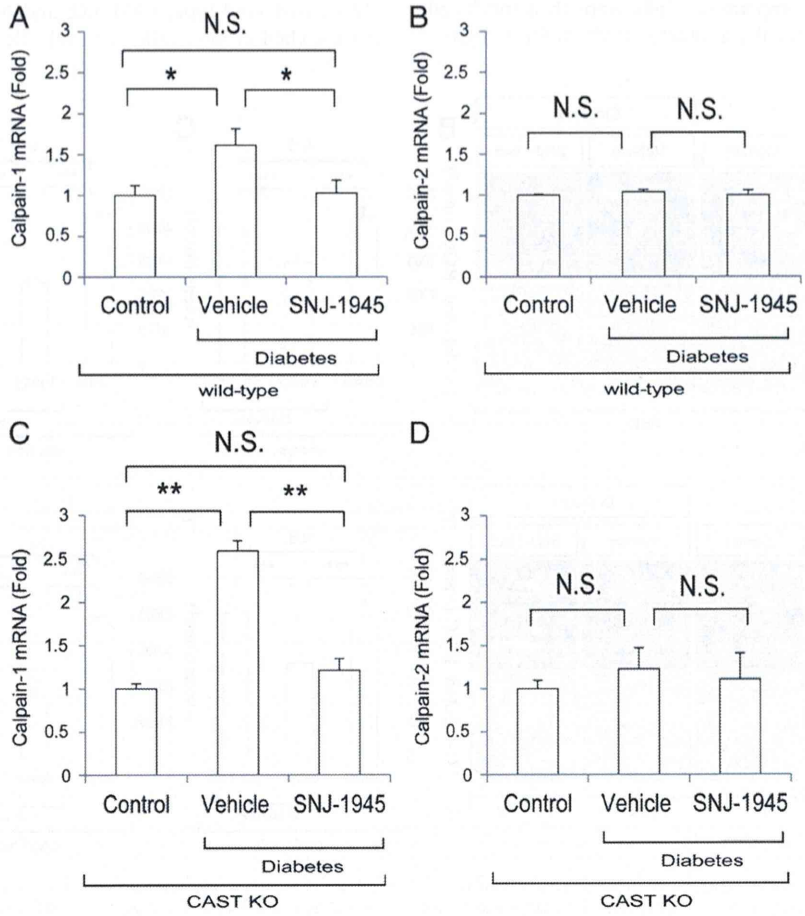

Fig. 4. Calpain-1 but not calpain-2 was activated in HFD and STZ-induced hyperglycemia. (A–B wild-type mice; C–D CAST KO mice) Bar charts showing the quantitative data from qRT-PCR in the neural retina with specific primer sets for calpain-1 and calpain-2 4-weeks after HFD- and STZ-induced hyperglycemia ($n = 6$ each condition). N.S.: no significance. *$p<0.05$, **$p<0.01$ vs. control.

4-weeks of HFD- and STZ-induced hyperglycemia. Combined with higher neuro-degeneration in the CAST KO mice compared to the wild-type mice, this indicated that calpain is a leading cause of RGC death in HFD–hyperglycemia induced retinopathy, and that SNJ-1945 protected RGCs and their axons in both diabetic wild-type and CAST KO mice.

HFD- and hyperglycemia-induced calpain activation in mouse retinas

To investigate the role of the calpain pathway in the retina, we evaluated the gene expression in our model of calpain-1 and calpain-2 in the retina 4-weeks after treatment with STZ in mice fed a HFD. qRT-PCR data showed that there was a significant increase in the mRNA expression of calpain-1 levels in STZ-treated animals of both wild-type ($p=0.023$) and CAST KO ($p=0.005$) compared to those treated with citrate buffer (Fig. 4A, C). Orally administrated SNJ-1945 significantly suppressed the upregulation of gene expression of calpain-1 in both wild-type ($p=0.023$) and CAST KO mice ($p=0.005$) compared to STZ-treated ones, almost bringing them back to normal. However, there was no significant difference in the gene expression of calpain-2 compared to the control in either treated group (Fig. 4B, D). These data showed that gene upregulation of calpain-1, but not calpain-2, was responsible for inducing RGC toxicity in our diabetic model, and that the gene expression of calpain-1 was downregulated by the administration of SNJ-1945.

Cleavage of α-fodrin targeted ganglion cell death was suppressed with SNJ-1945

Since expression of the calpain-1 gene was up-regulated, we tried to determine whether cleaved α-fodrin could be detected in the retina 4-weeks after treatment with STZ. Immunoblot analysis demonstrated that cleaved α-fodrin was significantly increased in STZ-treated wild-type ($p=0.029$) and STZ-treated CAST KO mice ($p=0.024$) compared to a citrate buffer-treated control group (Fig. 5A–B wild-type, C–D CAST KO). We next tried to modify the status of the activated calpain by orally administering SNJ-1945 at 100 mg/kg/day in our diabetic mice. The level of band intensity of cleaved α-fodrin decreased after SNJ-1945 treatment in the wild-type and CAST KO mice ($p=0.981$, 0.937 respectively), approaching the control groups (Figs. 5A–B, C–D). These data suggest that activated calpain-1 in STZ-treated animals led to autolytic cleavage of α-fodrin into its large pro-apoptotic products at 150 kDa, which induced RGC death. SNJ-1945 was able to suppress the band intensity of cleaved fodrin, bringing it close to normal.

Reduction of RGC density and synaptophysin in the diabetic retina was reversed by SNJ-1945

To understand the underlying mechanism of how calpain activation led to RGC degeneration in our diabetic mouse model, having already determined the cause of axonal degeneration, we evaluated the expression of C38 (MB88), an antigen that is specifically expressed in RGCs (Wakabayashi et al., 2010). We also evaluated their cell transduction by examining synaptophysin, a synaptic vesicle protein abundant in the inner retinal neurons (Kurihara et al., 2008). RGC count was significantly decreased in the STZ-treated groups compared to the control citrate buffer groups and STZ-SNJ-1945 groups (Fig. 6A—left panels, C). Interestingly, synaptophysin protein levels also decreased significantly in retinas with hyperglycemia compared to the control (Fig. 6E), especially in the inner plexiform layer (IPL), at the four-week point of the experiment (Fig. 6A—right panels). SNJ-1945 significantly blocked the decrease of synaptophysin protein in the

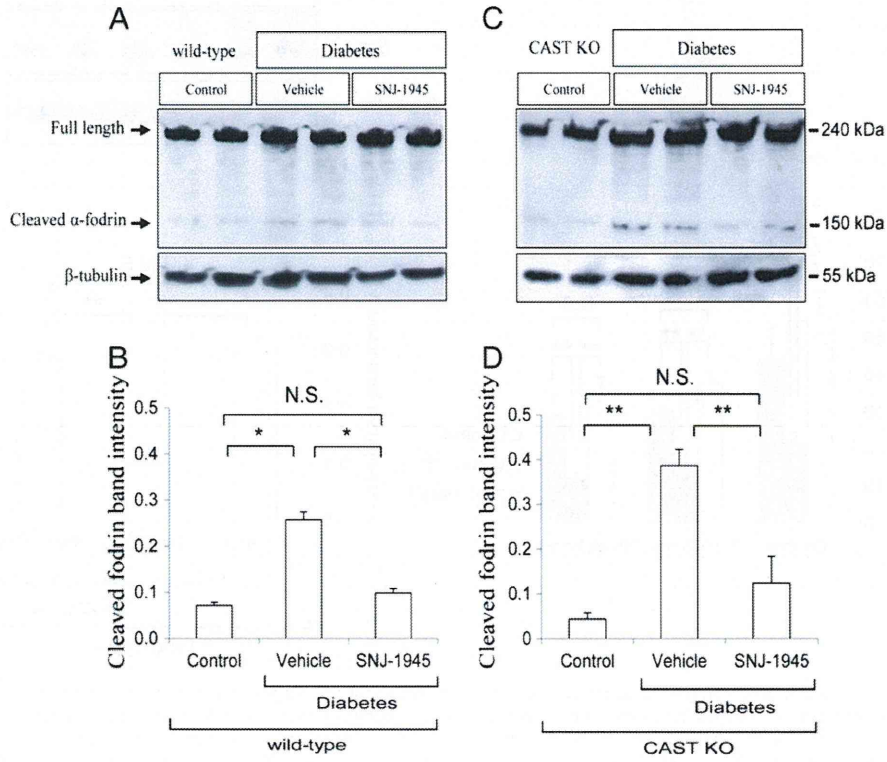

Fig. 5. SNJ-1945 suppressed the cleaved α-fodrin of HFD and STZ-induced hyperglycemia. (A, C) Photographs representing immunoblot analysis. They show the band density of cleaved α-fodrin 4-weeks after the induction of diabetes. (B, D) Quantitative data for the bands representing cleaved fodrin ($n=4$ each group) in wild-type (B) and CAST KO (D) mice. The cleavage of fodrin into its pro-apoptotic products at 150 kDa is generated through the activation of calpain, which was suppressed significantly with SNJ-1945. The density values of cleaved α-fodrin were normalized to density values of β-tubulin. N.S.: no significance. *$p<0.05$, **$p<0.01$ vs. control.

retina (Fig. 6D–E). These data suggested that a loss in synaptic vesicle input might occur in DR, linked to calpain activation. SNJ-1945 administration rescued RGCs and their synapses from diabetic pathological changes.

SNJ-1945 suppresses oxidative stress-induced RGC death in vivo

We next investigated the role of oxidative stress in inducing RGC death, including the role of calpain activation. We induced hyperglycemia

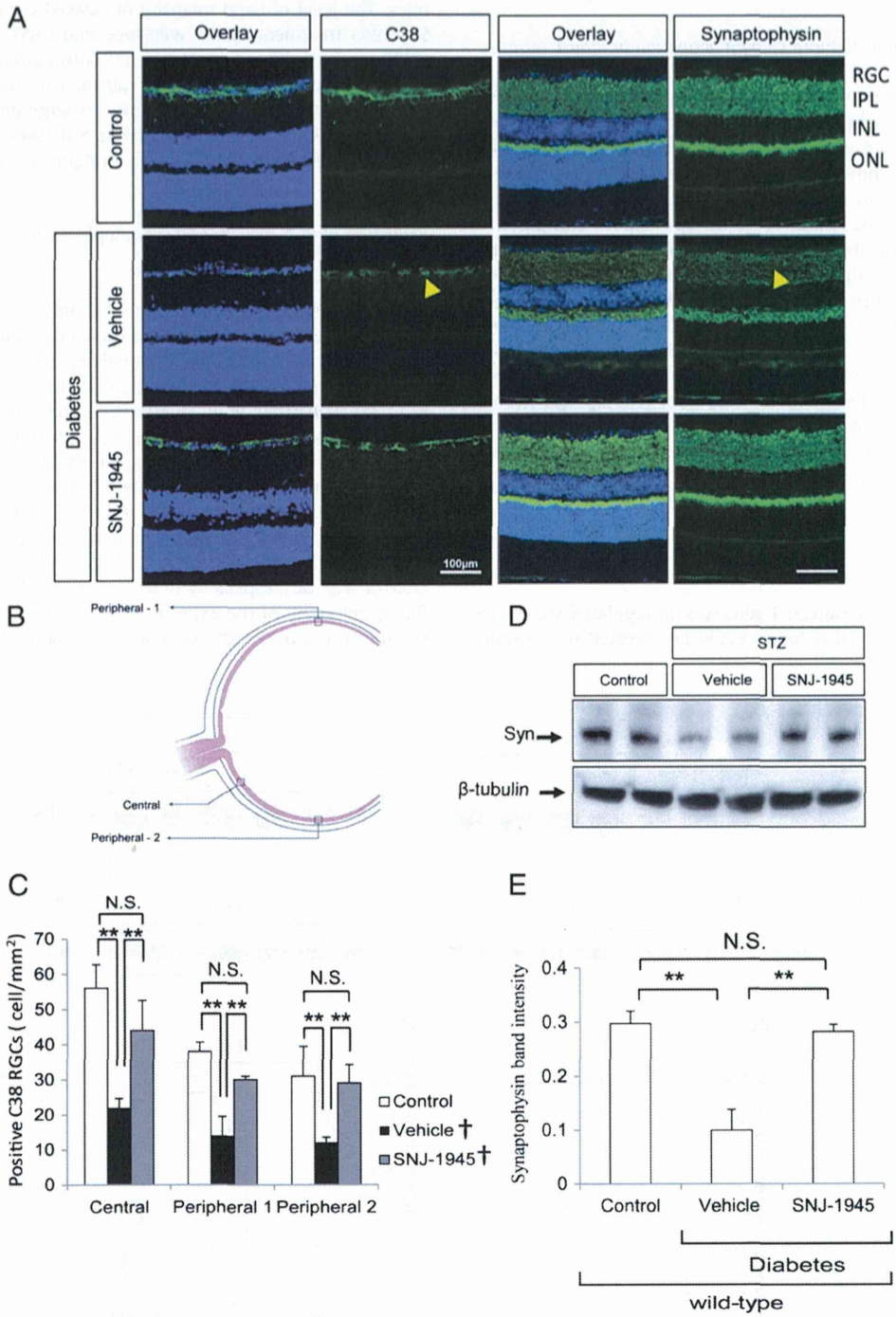

Fig. 6. SNJ-1945 prevented the HFD- and hyperglycemia-induced reduction of RGC and synaptophysin. (A) Representative photomicrographs of retinal sections immunostained with antibody against C38 (upper left panels), synaptophysin (upper right panels) and double labeling (overlap) with DAPI nuclear staining. The yellow arrowheads show a coincident decrease in both positive C38 RGC expression (left middle panel) and synaptophysin (right middle panel), and immunoreactivity in the inner plexiform layer (IPL) in the diabetic mice, compared to those treated with SNJ-1945. (B) Illustrated diagram of a cryosectioned eyecup showing the positions of the microscopic captures. (C) Quantitative data for the number of positive C38 RGCs (n = 16 in each condition). (D) Representative photographs of immunoblot analysis with synaptophysin (Syn: upper panel) and β-actin (lower panel) 4-weeks after induction of diabetes with and without SNJ-1945. (E) Quantitative data for the band intensity ratio of synaptophysin to β-tubulin (n = 4 each condition). The figures show that SNJ-1945 prevented HFD- and hyperglycemia-induced reduction in RGCs and synaptophysin protein. †STZ-treated group, N.S.: no significance. **$p<0.01$ vs. control.

in Nrf2 KO mice fed a HFD and over the course of 4-weeks (Fig. 7). Nrf2 is a key transcript factor for the expression of antioxidant genes, such as glutathione and HO-1, and protects against oxidative stress. Our data showed a significant decrease in the density of FG-labeled RGCs at week four in STZ-treated Nrf2 KO mice (2312 ± 212 cells/mm^2, $p<0.0001$), compared to wild-type mice treated with citrate buffer (3746 ± 115 cells/mm^2) (Fig. 7A–B). The survival rate of RGCs was 58.2% at week four, suggesting that oxidative stress is also involved in the pathogenesis of hyperglycemia-induced RGC death. Since it has been reported that oxidative stress increases intracellular free Ca^{2+} levels, and activates Ca^{2+}-dependent enzymes (Ray et al., 2000), we evaluated calpain status in Nrf2 KO mice retinas at the four week mark of the experiment by investigating the state of α-fodrin. Immunoblot analysis demonstrated that cleaved α-fodrin increased significantly in STZ-treated mice ($p=0.004$) compared to animals treated with the citrate buffer. The cleavage of fodrin was significantly ($p=0.004$) reduced in STZ-treated mice with administration of SNJ-1945 compared to vehicle groups (Fig. 7C–D). Interestingly, SNJ-1945 also significantly suppressed RGC death after just 2-weeks of administration (Fig. 8A–B). These data revealed that oxidative stress is involved in inducing RGC death in our diabetic model, and that SNJ-1945 can significantly suppress RGC degeneration by preventing subsequent calpain activation (Fig. 1).

Hyperglycemia-induced RGC death was mediated by oxidative stress and the SNJ-1945 had a neuroprotective effect in vitro

Measuring free radicals in animal models is difficult because of their transient nature, but since the production of free radicals is closely associated with hyperglycemia in cell culture models (Mullarkey et al., 1990), we tried to evaluate the state of oxidative stress on cultured RGCs (Fig. 9) in a high-glucose culture medium, using an anti-oxidant supplement with or without SNJ-1945. In a high glucose culture medium without an anti-oxidant supplement, the density of surviving βIII-tubulin (+) RGCs decreased significantly ($1.1 \pm 0.5\%$, $p<0.0001$) compared to cultures treated with anti-oxidants ($6.3 \pm 1.2\%$). SNJ-1945 (40 μM) significantly suppressed RGC death ($4.5 \pm 0.3\%$, $p<0.0001$) (Fig. 9A–B). When anti-oxidants and SNJ-1945 were combined, there was a significant ($8.6 \pm 0.6\%$, $p=0.0271$) additive neuro-protective effect compared to cultures treated with only anti-oxidants. These data give clear evidence that calpain and oxidative stress participate in hyperglycemia-induced RGC death. Together, anti-oxidants and calpain inhibitors provide potent neuroprotection against hyperglycemia-induced RGC toxicity.

Discussion

RGCs are the main output neurons in the retinal visual pathway and direct dysfunction of RGCs influences a patient's visual function. Thus, RGCs are an important cellular target for neuro-protective treatment to prevent blindness in patients with DR. This study was designed to investigate the neurotoxic effect on RGCs of combining a high fat diet (HFD; as a source of lipid peroxidation) (Park et al., 2010), and hyperglycemia, induced by frequent low doses of STZ.

Our data showed that a HFD and hyperglycemia caused a significant increase in RGC degeneration, including the synapse and axon, at the four-week mark of the experiment. In CAST KO mice, which

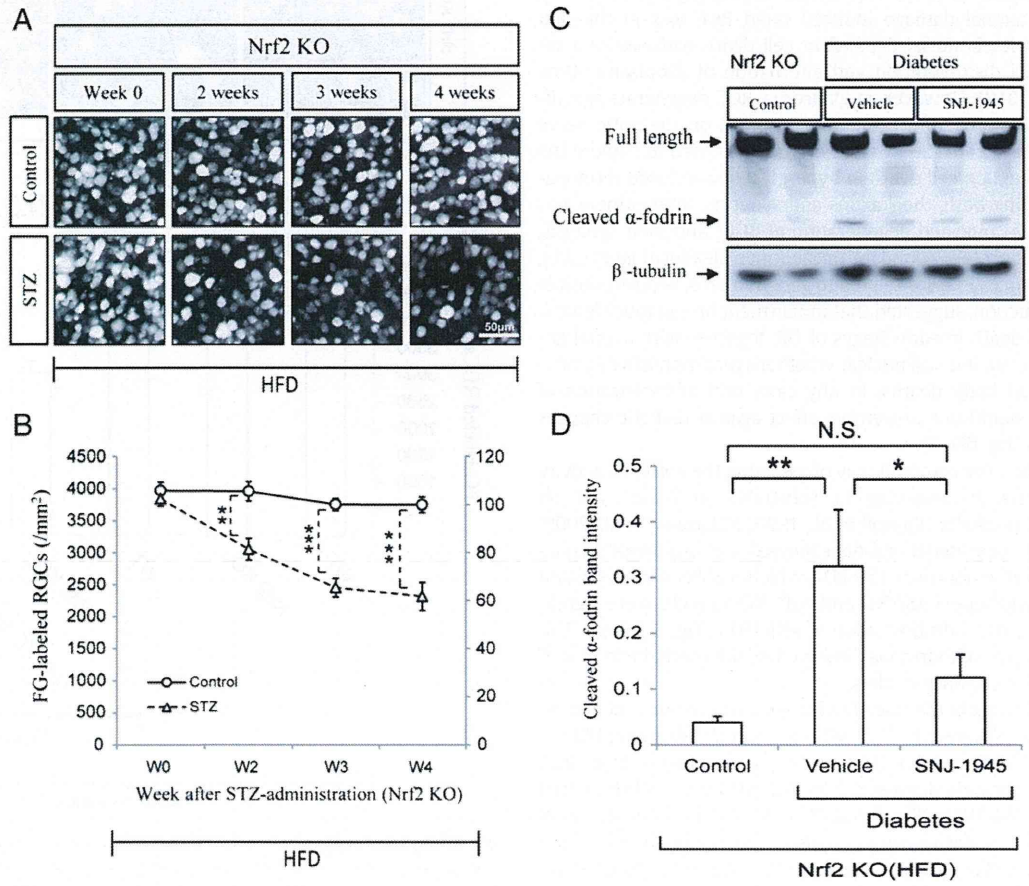

Fig. 7. Nrf2 deficiency in mice treated with STZ induced RGC degeneration; SNJ-1945 prevented cleavage of fodrin. (A) Representative photos of fluorogold (FG)—back labeled RGCs in flat-mounted Nrf2 KO mouse retinas after 4-weeks. (B) Quantitative data for FG-labeled RGCs ($n=6$ each time point). (C) Photographs of immunoblot analysis, showing that band intensity was significantly up-regulated in STZ-treated mice compared to mice treated with citrate buffer and SNJ-1945. (D) Bar chart showing the band density of cleaved fodrin ($n=4$ each group), normalized to the density of β-tubulin. N.S.: no significance, *$p<0.05$, **$p<0.001$, ***$p<0.0001$ vs. control. Circles = control, triangles = STZ.

are susceptible to calpain activation, hyperglycemia-induced RGC death was higher earlier on, at the two-week mark, compared to wild-type mice (Fig. 2B). These results indicate that calpain plays an important role in RGC degeneration.

The percentage of surviving RGCs in wild-type and CAST KO mice is close in week four, but this may be explained as calpastatin showed only a limited, weak neuroprotective effect; it suppressed RGC death during only the first 2-weeks following STZ induction in wild-type mice fed a HFD. Noting this, we attempted to suppress calpain activation by using a more potent exogenous calpain inhibitor, SNJ-1945, an α-ketoamide derivative containing a secondary amine in place of the cyclopropyl ring. This increases the potency of calpain inhibition by ten times (Cuerrier et al., 2006), with the advantage that it can cross the blood–retinal barrier (Shirasaki et al., 2006). However, it shows a protective effect on cultured human retinal endothelial cells (Ma et al., 2009). After induction of hyperglycemia, RGC and axonal degeneration was successfully prevented by SNJ-1945 4-weeks into the experiment (Fig. 3).

It has been reported that mRNA expression of calpain is correlated with its activity (Li et al., 2009; Muroya et al., 2012). SNJ-1945 was able to suppress mRNA overexpression of calpain-1 in our diabetic model (Fig. 4), which may be explained by the changing shape of calpain shifting domains to form an active compact structure, affecting mRNA expression (Suzuki et al., 2004). However, SNJ-1945 prevents these structural changes, and is thus responsible for keeping mRNA expression of calpain-1 close to normal.

A recent publication by our team concluded that orally administered SNJ-1945 protects against RGC degeneration induced by optic nerve crush and vinblastine in an in vivo mouse model (Ryu et al., 2011). Those types of axonal damage induced rapid RGC loss in the first 7-days, with a mitochondrial-dependent cell death pathway as a response to a rapid disintegration and alternation of axoplasmic flow (Knoferle et al., 2010). However, in glaucoma, RGC degenerate specifically from axonal damage in the lamina cribrosa on the optic nerve (Kerrigan-Baumrind et al., 2000). In this study, we tried to explore the mechanism of ganglion cell death in hyperglycemia-induced retinopathy by investigating both, their axons and synapsis. Interestingly, our data had shown a coincided degeneration of RGCs and their synapsis, a synaptic vesicle protein abundant in the inner plexiform layer (IPL), mainly representing synapses related to ganglion cells, and responsible for signal transduction, suggested that impairment on synaptic signal is involved in RGC death in early stages of DR, together with axonal degeneration. However, it is still unclear whether synaptophysin degradation precedes cell body deaths. In any case, oral administration of SNJ-1945 had a significant preventive effect against diabetic changes to RGC synapses (Fig. 6D–E).

In many studies, the common way of assessing the autolytic activity of calpain is through measuring its substrates (α-fodrin), and its break-down end products (Kampfl et al., 1996; Nakazawa et al., 2009; Nath et al., 1996). Our model and data showed that pro-apoptotic end products of cleaved α-fodrin at 150 kDa, which had been up-regulated in STZ-treated wild-type, CAST KO and Nrf2 KO animals, were significantly reduced by oral administration of SNJ-1945 (Fig. 5, 7C–D). This reveals that cleavage of fodrin was involved in the mechanism of RGC death in our diabetic mouse models.

In our investigation of the role of oxidative stress in our experiment, we induced hyperglycemia in Nrf2 KO mice, which are susceptible to oxidative stress. We found that HFD- and hyperglycemia-induced RGC deaths were significantly augmented in Nrf2 KO mice, and decreased significantly by SNJ-1945 (Fig. 7A–B, 8 A–B). Previous reports have documented that oxidative stress increases intracellular free Ca^{2+} levels, and activates Ca^{2+}-dependent enzymes (Ray et al., 2000). In response, we evaluated the link, if any, between oxidative stress and calpain activation in a high glucose culture medium with or without antioxidants in an in vitro retinal experimental model (Fig. 9). Our data has shown a significant neurodegenerative influence of RGCs 24 hr after incubation in a high glucose (45 mM D-glucose) culture without antioxidant (AO−), compared to those treated with antioxidant supplement (AO+). These results suggested that oxidative stress was induced in high glucose culture medium and participated in pathogenesis of RGCs death. Then, we evaluated the condition of the high glucose culture medium with (40 μM) SNJ-1945. It has significantly protected RGCs against high glucose-induced oxidative stress, when compared to the non-treated groups (Fig. 9B). The neuroprotective effect of SNJ-1945 was weaker than that of the antioxidants in vitro because the antioxidants were a mixture of potent antioxidant compounds. This does not imply that activation of the calpain-signal was not involved in the RGC death. However, the influence which SNJ-1945 inhibits in high-glucose conditions, and in the presence of antioxidants, may be a remnant of oxidative stress that has not been canceled by the antioxidants, or may be another cell death pathway (i.e. ER stress). These data suggest that

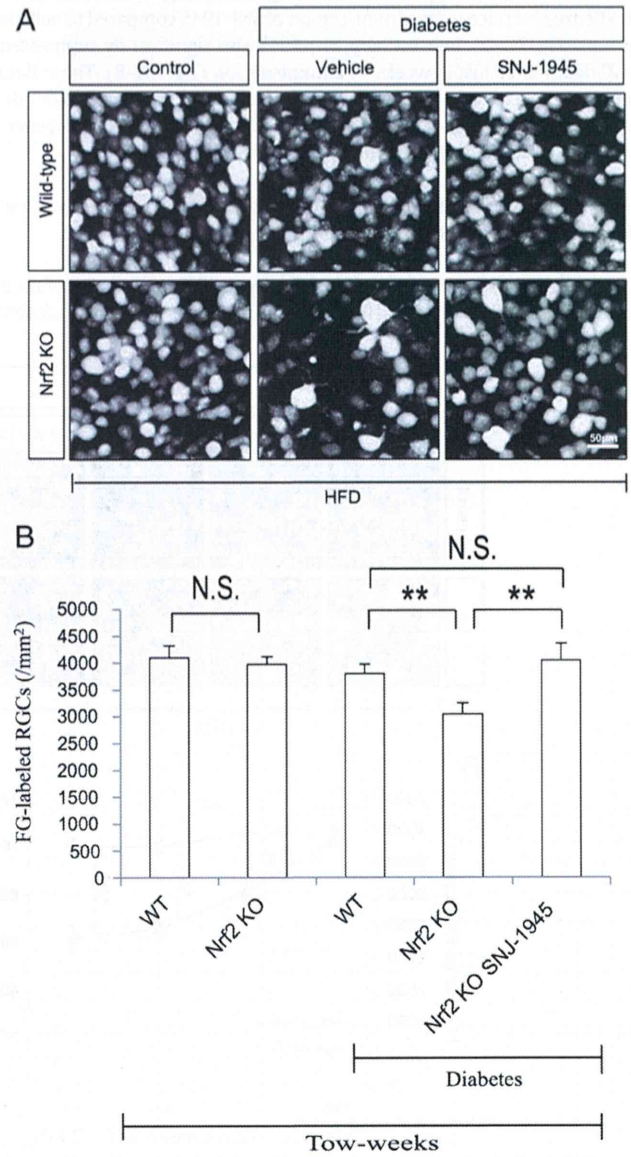

Fig. 8. SNJ-1945 suppressed oxidative stress induced RGC-degeneration in vivo. (A) Representative photos of positive FG-labeled RGCs in flat-mounted retinas, showing a dramatic decrease in RGCs in diabetic Nrf2 KO mice compared to non-diabetic wild-type mice. (B) Quantitative data of FG-labeled RGC density showing a significant degeneration in number of RGCs compared to wild-type and Nrf2 KO SNJ-1945-treated mice 2-weeks after STZ-induced hyperglycemia. Data represented mean ± SEM. N.S.: no significance. **$p<0.001$ vs. control.

oxidative stress induced by hyperglycemia is involved in the pathogenesis of RGC death, and that calpain inhibitors have the potential to protect RGCs against hyperglycemia-induced RGC toxicity.

At the cellular level, the mechanism of RGC death in our diabetic model is hypothesized to be due to hyper-excitability of the cell membrane, which occurs in hyperglycemia and leads to cell membrane depolarization and a Ca^{2+} influx through the voltage sensitive Ca^{2+} channel. Once inside the cell, the excitation of ER and mitochondria through an increase in oxidative stress hints at a release of more intracellular Ca^{2+}. Subsequently, calpain activation and cleavage of α-fodrin into pro-apoptotic end products will lead to cell deaths (Fig. 1).

In conclusion, calpain plays a curtailed role in HFD-induced RGC death caused by hyperglycemia and oxidative stress. Inhibition of calpain and the administration of antioxidants have the potential to prevent neuronal dysfunction in the early stages of vision threatening DR.

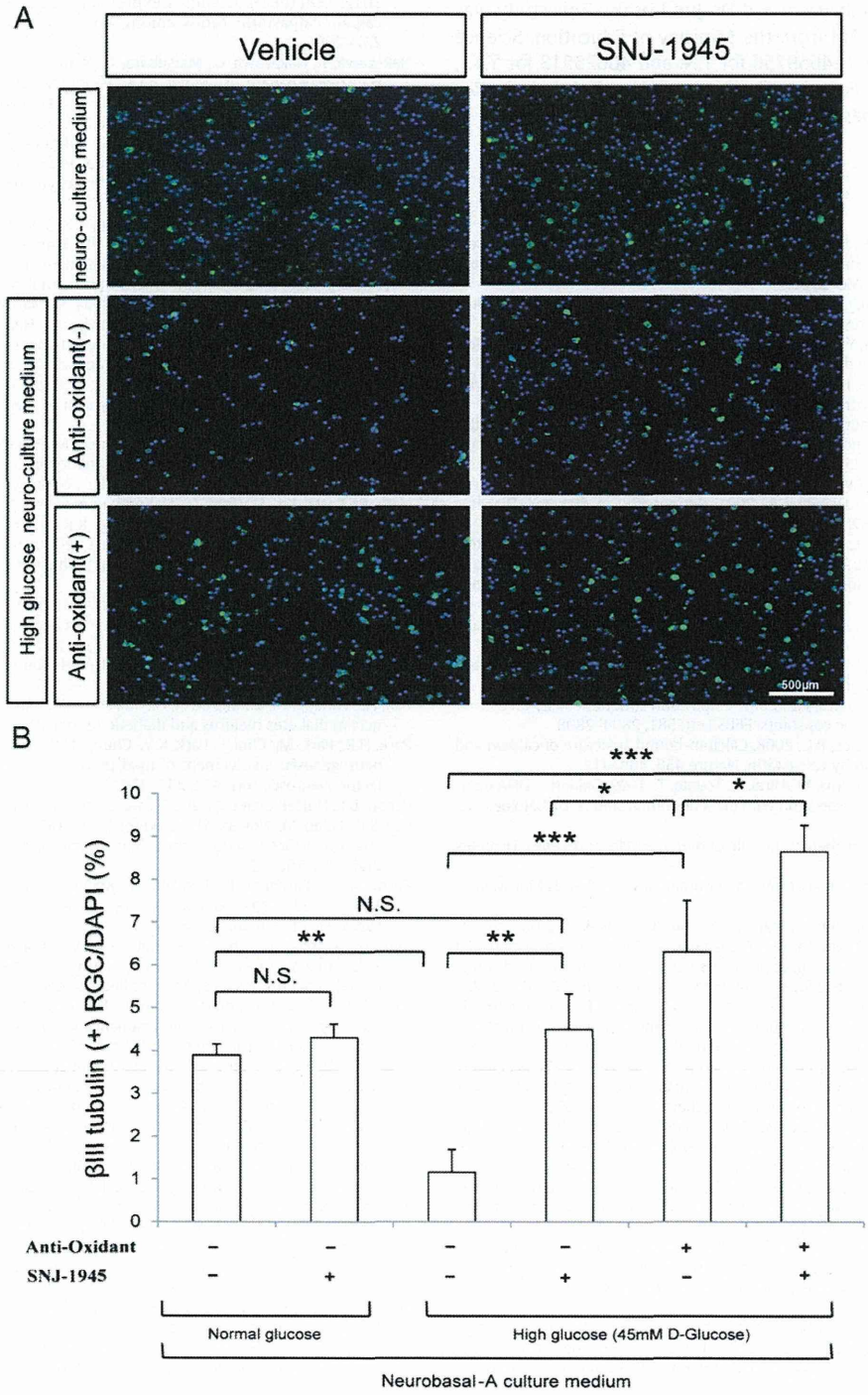

Fig. 9. Hyperglycemia-induced RGC death was mediated by oxidative stress and the neuro-protective effect of SNJ-1945 in vitro. (A) Representative photomicrographs of βIII tubulin-positive RGCs, normal sugar neurobasal-A culture medium with or without SNJ-1945 (upper panels). High sugar (45 mM D-glucose) neurobasal-A culture medium without anti-oxidant (middle panels) or with anti-oxidant (lower panels). SNJ-1945 (40 μM in final) was added to the groups on the right, and 0.1% DMSO to the vehicle. (B) Quantitative data for surviving RGCs 24 hr after culture (% of βIII tubulin-positive RGCs to DAPI). Data represented mean ± SEM. N.S.: no significance. *$p<0.05$, **$p<0.01$, ***$p<0.001$ vs. control.